

Dielectric elastomer actuators with elastomeric electrodes

Michael Bozlar, Christian Punckt, Sibel Korkut, Jian Zhu, Choon Chiang Foo et al.

Citation: *Appl. Phys. Lett.* **101**, 091907 (2012); doi: 10.1063/1.4748114

View online: <http://dx.doi.org/10.1063/1.4748114>

View Table of Contents: <http://apl.aip.org/resource/1/APPLAB/v101/i9>

Published by the [American Institute of Physics](#).

Related Articles

Acoustophoretic microfluidic chip for sequential elution of surface bound molecules from beads or cells
Biomicrofluidics **6**, 034115 (2012)

Graphene cantilever beams for nano switches
Appl. Phys. Lett. **101**, 093111 (2012)

High-Q gold and silicon nitride bilayer nanostrings
Appl. Phys. Lett. **101**, 093105 (2012)

Nanostructured anatase-titanium dioxide based platform for application to microfluidics cholesterol biosensor
Appl. Phys. Lett. **101**, 084105 (2012)

Shrunk to femtolitre: Tuning high-throughput monodisperse water-in-oil droplet arrays for ultra-small micro-reactors
Appl. Phys. Lett. **101**, 074108 (2012)

Additional information on *Appl. Phys. Lett.*

Journal Homepage: <http://apl.aip.org/>

Journal Information: http://apl.aip.org/about/about_the_journal

Top downloads: http://apl.aip.org/features/most_downloaded

Information for Authors: <http://apl.aip.org/authors>

ADVERTISEMENT



HAVE YOU HEARD?

Employers hiring scientists
and engineers trust
physicstoday JOBS



<http://careers.physicstoday.org/post.cfm>

Dielectric elastomer actuators with elastomeric electrodes

Michael Bozlar,^{1,a)} Christian Punckt,^{1,2,a)} Sibel Korkut,^{1,2} Jian Zhu,³ Choon Chiang Foo,^{3,4} Zhigang Suo,³ and Ilhan A. Aksay^{1,b)}

¹Department of Chemical and Biological Engineering, Princeton University, Princeton, New Jersey 08544, USA

²Vorbeck Princeton Research Center, Vorbeck Materials Corp., 11 Deerpark Drive, Monmouth Junction, New Jersey 08852, USA

³School of Engineering and Applied Sciences, Harvard University, Cambridge, Massachusetts 02138, USA

⁴Institute of High Performance Computing, 1 Fusionopolis Way, #16-16 Connexis, Singapore 138632, Singapore

(Received 24 May 2012; accepted 9 August 2012; published online 29 August 2012)

For many applications of dielectric elastomer actuators, it is desirable to replace the carbon-grease electrodes with stretchable, solid-state electrodes. Here, we attach thin layers of a conducting silicone elastomer to prestrained films of an acrylic dielectric elastomer and achieve voltage-actuated areal strains over 70%. The influence of the stiffness of the electrodes and the prestrain of the dielectric films is studied experimentally and theoretically. © 2012 American Institute of Physics. [<http://dx.doi.org/10.1063/1.4748114>]

Since Pelrine and coworkers showed that large deformations of up to 158% areal strain can be achieved with electrostatic actuators based on prestrained acrylic elastomer films,¹ polymer-based actuators, often referred to as dielectric elastomer (DE) actuators, gained an increasing attention in the scientific community.^{2–9} Both experimental and theoretical studies have been carried out over the last 12 years to investigate the fundamental properties of such devices,^{2,4,6,7,9} and numerous potential applications ranging from artificial muscles,⁷ to optical components,^{3,5,8} have emerged.

An important factor governing the performance of DE actuators is the nature of the electrodes.^{7,10,11} The electrodes need to exhibit sufficient electrical conductivity (typically on the order of 10^{-7} S/m for actuation on a time scale of 1 s) and low elastic modulus (compliance) not to impede actuation. They must also adhere to the dielectric film to prevent slippage between the electrode and the dielectric film during actuation and to provide mechanical integrity for the overall assembly. Compliant electrodes made of carbon grease or graphite powder have been commonly used in most experimental studies because they combine electrical conductivity with negligible elastic modulus.¹¹ Despite enabling high actuation amplitudes, these electrodes exhibit poor structural stability which constrains the integration of such actuators into other systems. All-polymeric actuators with “solid” composite elastomer electrodes can overcome such limitations while providing actuation with practically relevant amplitude.^{3,8,12} Moreover, while actuators with fully compliant electrodes have to rely on a rigid frame to maintain the prestrain of the dielectric membrane, the use of solid electrodes may enable the development of frame-free actuators: When released from the frame, the dielectric membrane retains a fraction of its prestrain while the electrodes are compressed. This is expected to lead to an improved actuation performance compared to non-prestrained frameless actuators, similar

to what has been observed in studies with interpenetrating polymer networks.¹³

To date, no systematic studies have been conducted to understand the limitations imposed by solid electrodes on the performance of DE actuators. In this Letter, we report on model simulations of DE actuators with solid electrodes of varying stiffness and compare these with actuators comprised of VHB 4910 acrylic DE film^{4,14} (3 M, St. Paul, MN) and crosslinked carbon black/poly(dimethylsiloxane) (CB/PDMS) conducting elastomer (CE) electrodes. The acrylic DE film was chosen based on its low shear modulus of 73 kPa (determined from a measurement of Young’s modulus) and over 800% linear strain before failure, which makes it a popular choice for DE actuators (Table I). The PDMS-based CE electrodes exhibit a comparably large shear modulus of 300 kPa (Table I) and thus impose significant mechanical impedance on the mechanical response during actuation tests if they have a thickness comparable to that of the DE. We measured that they provide conductivities of 0.1 to 10^{-3} S/m in the range from 0 to 100% linear strain and do not fail mechanically up to about 150% linear strain, which is a sufficient strain level for actuator applications. The mechanical properties of DE and CE films are summarized in Table I. In the following, we show that replacing fully compliant (e.g., carbon grease) electrodes with stiff elastomeric ones yields actuators with qualitatively the same performance characteristics that can still achieve areal strains up to 77%.

For our simulations, we consider the actuation of a perfectly dielectric membrane under equi-biaxial prestrain, as shown in Figure 1(a). In the reference state, the square DE

TABLE I. Mechanical properties of DE (VHB 4910) and CE (CB/PDMS) composites with 3 wt. % CB concentration, cured at 70 °C. Uniaxial tensile tests were performed at a strain rate of $\approx 4\%/s$, on 4 dogbone samples for each material, and the maximum achieved strain at failure is reported.

Specimen	Young’s modulus (kPa)	Shear modulus (kPa)	Strain at failure (%)
VHB 4910	220	73	860
CB/PDMS	910	300	148

^{a)}Michael Bozlar and Christian Punckt contributed equally to this work.

^{b)}Author to whom correspondence should be addressed. Electronic mail: iaksay@princeton.edu.

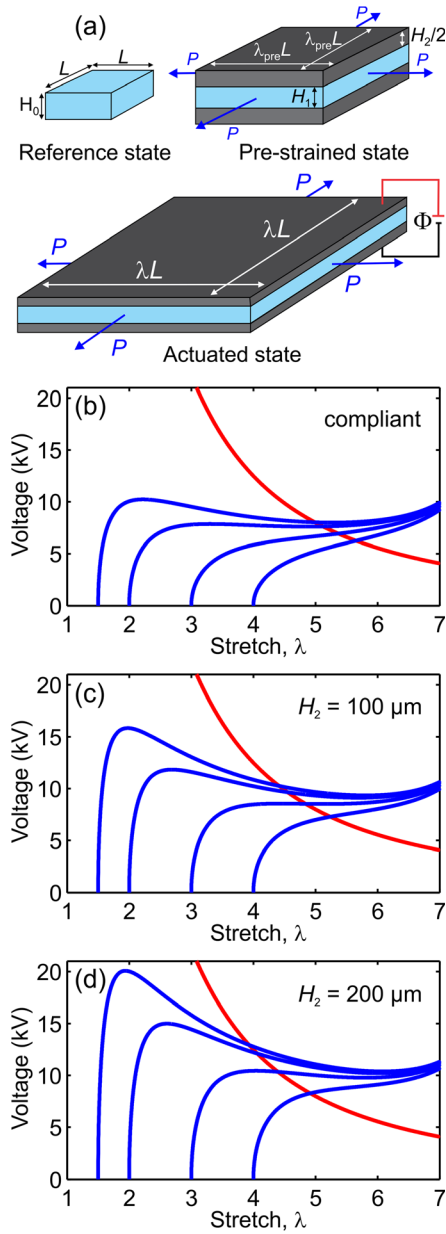


FIG. 1. (a) Schematics of DE actuator in different states. (b)–(d) Mechanical response of DE membranes with electrodes of different stiffness. The red curves correspond to the electric breakdown limit of 200 MV/m. (b) Perfectly compliant electrodes, (c) and (d) solid electrodes, $H_0 = 1$ mm.

membrane of length L and thickness H_0 is subject to no force and no voltage. In the prestretched state, subjected to an equi-biaxial force P , the membrane assumes a length $\lambda_{pre}L$ and a thickness H_1 . The prestretched membrane is in mechanical contact (no slip) with electrodes of combined thickness H_2 that exhibit no stress. In the actuated state, subject to both the force P and the voltage Φ , the membrane and the electrodes expand in area and decrease in thickness. With the changes in thickness being h and the length l , we define the following parameters: stretch $\lambda = l/L$, stress $\sigma = P/(lh)$, and the electric field $E = \Phi/h$. The membrane is taken to be incompressible, so that $H_1 = H_0\lambda_{pre}^{-2}$ and $h = H_0\lambda^{-2}$. DEs show pronounced strain-stiffening.¹⁴ To account for the effect of strain-stiffening on actuation, we write the stress-strain relation by adopting the Gent model.¹⁵ The equation of state takes the form¹⁶

$$\frac{P\lambda}{\lambda_{pre}^2 L(H_1 + H_2)} + \phi^A \varepsilon \left(\frac{\lambda^2 \Phi}{H_0} \right)^2 = \frac{\phi^A \mu^A (\lambda^2 - \lambda^{-4})}{1 - (2\lambda^2 + \lambda^{-4} - 3)/J_{lim}^A} + \frac{\phi^B \mu^B (\lambda^2 \lambda_{pre}^{-2} - \lambda^{-4} \lambda_{pre}^4)}{1 - (2\lambda^2 \lambda_{pre}^{-2} + \lambda^{-4} \lambda_{pre}^4 - 3)/J_{lim}^B}, \quad (1)$$

where $\phi^A = H_1/(H_1 + H_2)$ and $\phi^B = H_2/(H_1 + H_2)$, ε is the dielectric permittivity, μ^A the shear modulus of the DE film, and μ^B the shear modulus of the CE. J_{lim}^A and J_{lim}^B are constants related to the stiffening of the elastomer and the electrodes, respectively.¹⁷ This equation defines the stretch λ of a membrane subject to given values of P and Φ . The shear modulus of the DE film was chosen as $\mu^A = 50$ kPa, such that a good agreement between theory and actuation experiments (under prestrain) was observed. This value is lower than the one reported in Table I which is likely the case because of the higher strain rate used in tensile testing compared to strain rates typically achieved in actuation tests (see below). For the DE, $\varepsilon = 4.11 \times 10^{-11}$ F/m and the electric breakdown voltage $\Phi_{EB} = hE_{EB}$, with a constant value of the electric breakdown field set to $E_{EB} = 200$ MV/m. J_{lim}^A was set to a value of 125.¹⁸ The shear modulus of the CE electrodes was set to the experimentally determined value of $\mu^B = 300$ kPa, and we assumed a neo-Hookean stress-strain relation since the CE will not experience more than $\approx 30\%$ linear strain which results in $J_{lim}^B = \infty$.

We plot the electromechanical response of actuators with electrodes of different stiffness (Figs. 1(b)–1(d)). The behavior of an actuator with fully compliant electrodes (zero shear modulus) has been previously reported¹⁹ and is shown in Figure 1(b). At $\lambda_{pre} = 1.5$, the voltage-strain curve shows a local maximum before intersecting with the electrical breakdown curve, and the actuator fails by electromechanical instability once the local maximum of the curve is reached. The tangential shear modulus of the DE $\mu_{tangent}$ (at $\Phi = 0$ V) is reduced to 30.6 kPa due to the presence of the force P which contributes to the increase of the mechanical response of the actuator. Qualitatively, the same behavior is observed at $\lambda_{pre} = 2$. However, $\mu_{tangent}$ is slightly increased to a value of 38.1 kPa. At $\lambda_{pre} = 3$, the voltage-strain curve increases monotonically, and $\mu_{tangent} > 66$ kPa due to the hyperelastic characteristics of the DE. In this case, the maximum strain of actuation is limited by electric breakdown; and, due to elimination of the instability, the membrane can achieve large actuation strain. The transition from the occurrence of electromechanical instability to stable behavior occurs at $\lambda_{pre} \approx 2.3$.

The electromechanical responses of the actuators with solid electrodes of total thicknesses $H_2 = 100$ μ m and $H_2 = 200$ μ m are displayed in Figures 1(c) and 1(d), respectively. Not surprisingly, increasing the thickness (stiffness) of the CE electrodes results in smaller actuation strain at the same applied voltage. Similar to the case of fully compliant electrodes, as the prestrain of the dielectric membrane increases, actuators with solid electrodes exhibit a transition from unstable to stable behavior. However, this transition occurs at increasing levels of prestrain as the electrode thickness is increased ($\lambda_{pre} \approx 3.1$ for $H_2 = 100$ μ m and $\lambda_{pre} \approx 3.5$

$H_2 = 200 \mu\text{m}$). Thus, a DE actuator with solid electrodes only allows for large actuation amplitudes if λ_{pre} is sufficiently large and the electrode modulus is sufficiently small such that the electromechanical instability is suppressed. In other words, increasing the stiffness of the electrodes of an actuator operating in the electromechanically stable regime can render it unstable.

Using crosslinked CB/PDMS electrodes and prestrained DE membranes made from VHB 4910 acrylic adhesive film,^{4,14} we assembled actuator devices to put these theoretical results to an experimental test (Fig. 2). Depending on the desired thickness of the DE membrane, either a single layer or two stacked layers (double layer) of as-received 1 mm thick VHB adhesive were manually prestretched and attached to a cardboard frame with a 30 by 30 mm² opening. We prepared CB/PDMS composite CE electrodes with a CB concentration of 3 wt% following a recipe similar to the one previously established for graphene-reinforced conductive silicone elastomer electrodes (see Supplemental Material,²⁶ SM).⁸

Electromechanical testing of the actuators was done by applying triangular voltage ramps to the devices, such that viscoelastic effects are minimized. Simultaneously, images of the actuator were recorded with a CCD camera at a rate of about 0.35 Hz. After each actuation cycle, the sample was allowed to rest for a period of about 5 min until a subsequent voltage ramp was applied. More details about the experimental procedures can be found in the SM.

Figures 2(d)–2(g) show the mechanical response of an actuator with a DE double layer under 250% prestrain and solid CB/PDMS electrodes of 120 μm combined thickness. It was subjected to a voltage scan at a rate of 200 V/s up to a maximum voltage of 16 kV and back to 0 V. Snapshots of the actuator in the state of minimum and maximum extension during the course of the experiment are presented in Figures 2(d) and 2(e). From the change in electrode diameter d measured along the yellow lines (Figs. 2(d) and 2(e)), we calculate the linear (radial) actuation strain as $\epsilon_{\text{act}} = d/d_0 - 1$, where d_0 is the electrode diameter prior to application of the voltage. Also areal strain is calculated from the radial deformation of the actuator as $\epsilon_{\text{area}} = (d/d_0)^2 - 1$. This is done to reduce artifacts induced by the buckling of the actuator during the experiment (Fig. 2(e)), which renders data, obtained by measuring the projected surface area changes of the actuator directly, inaccurate: In the direction perpendicular to the buckles, the extension of the projected (apparent) electrode diameter is strongly reduced, while in the direction parallel to the wrinkles this error is less significant. We therefore analyze the linear actuator extension in a direction parallel to the buckles and thus reduce the error compared to a direct area measurement. The reduction of apparent actuator strain due to buckling is a well-known effect, which has already been described by Pelrine *et al.*¹ It has been attributed to mechanical instabilities of the actuator,²⁰ and sophisticated measurement techniques have been developed to account for this effect.²¹ Since the effect is well known and since the primary objective of this work is to investigate the impact of solid electrodes, buckling effects are not explored further and not taken into account in our model.

In Figure 2(f), we show applied voltage and ϵ_{area} as a function of time. While the voltage reaches its maximum

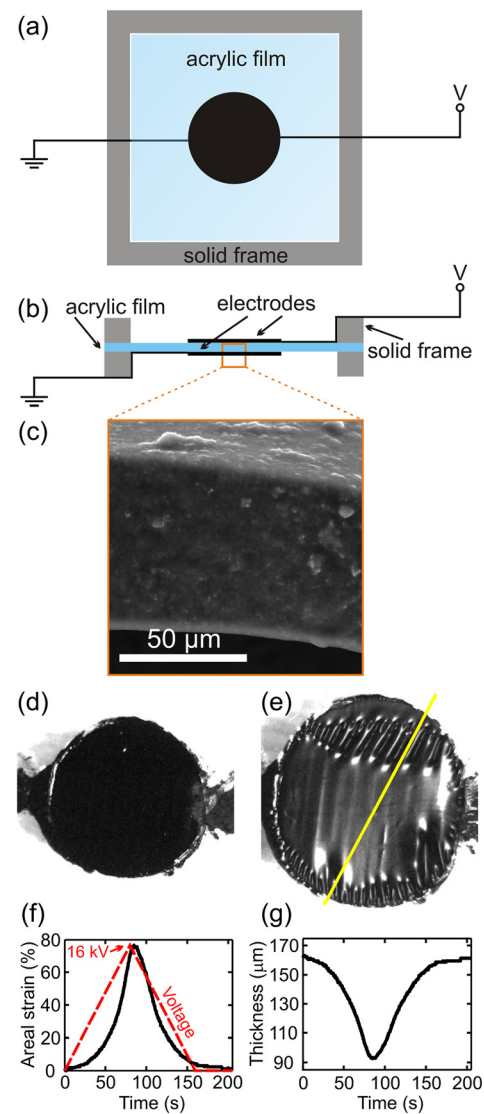


FIG. 2. Schematic of the actuator setup: (a) top and (b) side view. (c) Scanning electron microscope image displaying the magnified area corresponding to the cross section of the CB/PDMS composite CE electrode. (d), (e) Top views of the actuator at relaxed state and maximum actuation. (f) Areal strain as a function of time corresponding to the snapshots in (d), (e), the red dashed line represents the voltage protocol during the actuation cycle. (g) Thickness variation of the DE film as a function of time.

value of 16 kV at $t = 80$ s, maximum actuation of $\epsilon_{\text{area}} = 77\%$ is achieved at about $t = 85$ s. Thus, there is a temporal delay between the applied voltage and the mechanical response of the actuator. This effect can be attributed to the viscoelastic properties of the DE film.^{4,22,23} As a consequence of this phenomenon, the measurement of actuator properties depends on the time scale of the experiment (i.e., voltage scan rate). When using a triangular voltage protocol, maximum actuation is achieved neither at maximum applied voltage nor at maximum electric field as will be seen below. In order to determine the electric field experienced by the DE film, we calculate the change in DE film thickness h from the change in area assuming constant volume (Fig. 2(g)), and $E = \Phi/h$.

Results at two different scan rates for the actuator shown in Figures 2(d)–2(g) are compared in Figure 3(a), where we plot ϵ_{area} as a function of E . For any given applied electric field, at higher scan rate a smaller strain is achieved. The points where the maximum voltage of 16 kV is reached are marked

with red circles, indicating that both ϵ_{area} and, to a smaller degree, E continues to increase for a certain amount of time after the voltage scan direction is reversed. Once $E = 0 \text{ MV/m}$ is reached at the end of the cycle, a significant remanent strain is observed which slowly decays to zero within a few tens of seconds. These hysteresis effects are more pronounced in the case of high voltage scan rate. Accordingly, at 800 V/s , a maximum areal strain of only 61% is obtained, while at the smallest scan rate of 200 V/s , 77% strain is achieved. These observations emphasize that care needs to be taken to control hysteresis effects resulting from viscoelastic phenomena. While voltage scan rates smaller than 200 V/s reduce hysteresis further, we chose to conduct the tests described in the following at scan rates of 200 V/s , so that experiments were completed within a few minutes and actuator fatigue was minimized. In the following, we vary geometrical parameters of our actuators to show their impact on electromechanical response and compare these experimental results with model simulations for those specific actuator geometries.

By varying the thickness of the DE film, we can change the relative stiffness of the solid electrodes compared to the DE film without varying our electrode fabrication protocol. In Figure 3(b), we compare results obtained with single and double layer DE films under identical prestrain of 250%. Prior to actuation, the thickness of the single layer DE film was $82 \mu\text{m}$ and that of the double layer DE film was $163 \mu\text{m}$. We therefore reduced the scan rate in the experiment with the single layer film to 100 V/s so that viscoelastic effects, which depend on the strain rate, occur at a similar magnitude. The combined electrode thickness was $120 \mu\text{m}$ for both cases, resulting in electrode/DE thickness ratios of 1.5 and 0.7 for single and double layer DE, respectively. During test-

ing, the maximum applied voltage was increased from cycle to cycle in increments of typically 0.5 kV until eventually electrical breakdown occurred. The data shown correspond to the cycle with the maximum peak voltage that did not result in breakdown. Thus, the maximum electric field achieved during the actuation cycles in Figure 3(b) is representative of the breakdown field of the actuator. For a given value of E , the thicker DE film yields larger strain than the thinner film, because, due to the smaller thickness ratio, the electrodes cause less mechanical impediment to the extension of the DE. Further, both higher electric field and ultimate strain are achieved with the thicker DE layer.

In Figure 3(b), we also show ϵ_{act} as a function of electric field for an actuator with a double layer DE prestrained to only 150% and electrodes of $120 \mu\text{m}$ combined thickness. We observe that compared to the DE films with 250% prestrain, larger strain is achieved at equal electric field due to the small electrode/DE thickness ratio of 0.4. Additionally, lower prestrain results in a smaller value of μ_{tangent} , and the softer DE film is more easily compressible. On the other hand, the maximum strain is less than half the maximum strain of the actuators with highly prestrained DE. This is possibly the case because the softness of the film results in early failure due to electromechanical instability. Our experimental results are summarized in Table II.

To better understand the variations in actuator response, we performed numerical simulations with actuator geometries that correspond to the experimental configurations (Fig. 4). The results for the actuators with DE films of different thickness and 250% prestrain are compared in Figure 4(a). We find that theoretically no electromechanical instability is present. Consequently, the maximum strain is limited by the breakdown strength of the DE (red dots in Figure 4(a)). Both the theoretical result and the experiment show that larger ultimate strain can be achieved with the thicker DE film. Figure 4(b) shows that at lower prestrain of only 150% the electromechanical instability is not suppressed. The experimental curve initially follows the theoretical data but only reaches about 30% of the strain level that is expected from theory.

We hypothesize that the low values of maximum strain achieved in the experiments, in particular, in the case of Figure 4(b), are due to heterogeneities in the DE film and in the electrodes used for the experiments. These heterogeneities may be attributed to the manual pre-stretching procedure, potentially yielding variations in the thickness and structure of the DE film. In the case shown in Figure 4(b), an instability causing premature failure might have occurred locally prior to achieving a critical strain level globally. Since the breakdown strength of the DE film should exceed 200 MV/m , also the small

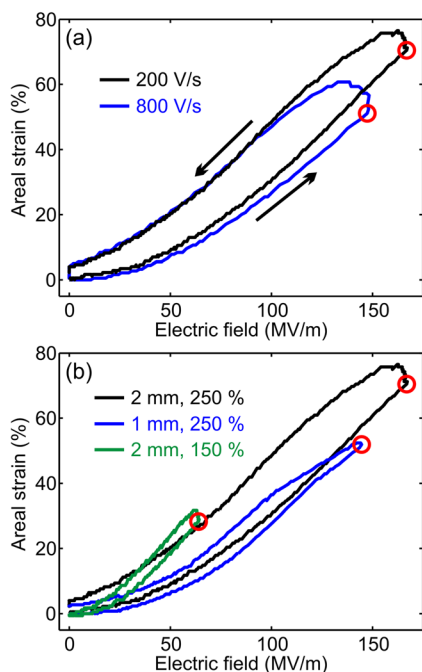


FIG. 3. Experimental actuation results with solid electrodes. The red circles indicate areal strain reached at maximum applied voltage. (a) Influence of voltage scan rate on the mechanical deformation of actuators with 250% prestrain. The arrows represent the voltage increase (up) and decrease (down) cycle. (b) Mechanical deformation as a function of electric field for actuators with two different prestrain levels and thicknesses.

TABLE II. Electromechanical properties of actuators with electrodes of $120 \mu\text{m}$ combined thickness and different DE film thickness and prestrain levels.

Prestrain (%)	DE film thickness H_1 (μm)	Voltage scan rate (V/s)	Max. areal strain (%)	Max. electric field (MV/m)
150	320	200	32	64
250	82	100	53	145
250	163	200	77	167
250	163	800	61	148

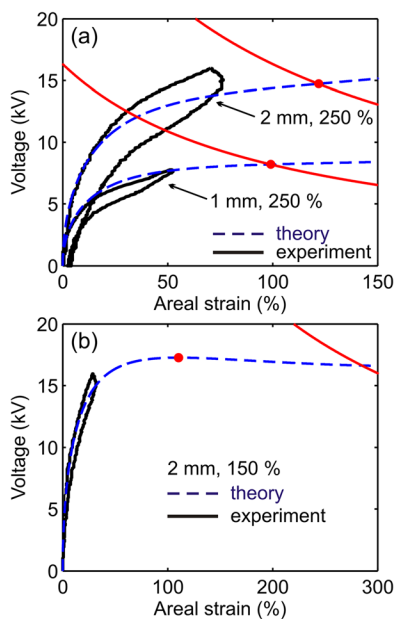


FIG. 4. Comparison of experimental and theoretical results with DE membranes of thickness and prestretch as indicated. Red curves correspond to the electric breakdown limit; red dots on the dotted blue curves represent the maximum achievable strain. A combined electrode thickness of $H_2 = 120 \mu\text{m}$ was used for the simulations.

maximum achievable experimental actuation in Figure 4(a) appears to indicate premature failure and may be related to such heterogeneities as well. Furthermore, it has been shown that under conditions similar to ours, prior to electrical breakdown, mechanical failure, i.e., stresses exceeding the mechanical strength of the DE film, may lead to the failure of the actuator in the case of high prestrain where the electromechanical instability is suppressed.²⁴

Another source of deviation between theory and experiments is the difference in the way prestrain is generated. Theory assumes that the membrane is subjected to homogeneous deformation under a constant (strain-independent) biaxial dead load.²³ This condition is not realized in the experimental setup as the DE film is constrained within a rigid frame (Fig. 2(a)). The presence of a rigid frame can be expected to impose a significant mechanical constraint onto the voltage-induced actuation of the active area and thus to cause apparent additional strain hardening. Furthermore, deformations in the passive regions of the DE film adjacent to the active area are not taken into account in the model, as they require the solution of a more complicated boundary-value problem.¹⁹ Lastly, the theory employed here assumes that the DE membrane is perfectly elastic and does not exhibit any strain rate dependence of its mechanical response, which is obviously not the case in the experiments.^{23,25} While these latter two aspects have been incorporated in theoretical models before,^{19,23,25} we decided to follow a more basic approach here, which yields qualitatively the same results. Using a more sophisticated model is not expected to cause a substantial improvement of the agreement between modeling and experiments as most of the observed deviations are due to experimental shortcomings discussed above. For tests that are targeted towards measuring the actuator response to voltage pulses, incorporating viscoelastic effects is not only necessary but may also yield additional insights into the effects of solid electrodes.

To summarize, we demonstrated that actuators with fully compliant and those with solid electrodes show qualitatively the same response to applied voltages. While the actuation amplitudes are reduced with solid electrodes, we still observe a transition from electromechanically unstable to stable characteristics, which allows for large actuation amplitudes. The dependence of the mechanical response on the prestrain level of the DE membrane, the ratio of electrode and DE thickness, and the voltage scan rate was studied experimentally, and we achieved a maximum areal strain of 77% with a double layer DE film at 250% prestrain and a voltage scan rate of 200 V/s. Despite the differences between the theoretical and the experimental settings, a reasonable quantitative agreement was observed between the experiments and model simulations. While the actuator performance is impeded by the presence of solid electrodes, their use offers advantages as well, such as structural stability, compatibility with more complex polymer systems, or the potential for frameless actuator designs. Solid electrodes therefore constitute a viable alternative to fully compliant but otherwise more limited electrode designs.

This work was supported by the Army Research Office Multidisciplinary University Research Institute (ARO/MURI) under Grant No. W911NF-09-1-0476. Additional support was provided by the Partner University Fund of the French American Cultural Exchange (PUF/FACE), sponsored by the French Embassy in the United States.

- ¹R. Pelrine, R. Kornbluh, Q. B. Pei, and J. Joseph, *Science* **287**, 836 (2000).
- ²F. Carpi and D. De Rossi, *Mater. Sci. Eng. C* **24**, 555 (2004).
- ³M. Aschwanden and A. Stemmer, *Opt. Lett.* **31**, 2610 (2006).
- ⁴M. Wissler and E. Mazza, *Sens. Actuators, A* **134**, 494 (2007).
- ⁵M. Becker, R. Fiolka, and A. Stemmer, *Opt. Lett.* **34**, 803 (2009).
- ⁶X. H. Zhao and Z. G. Suo, *Phys. Rev. Lett.* **104**, 178302 (2010).
- ⁷P. Brochu and Q. B. Pei, *Macromol. Rapid Commun.* **31**, 10 (2010).
- ⁸Z. H. Fang, C. Punckt, E. Y. Leung, H. C. Schniepp, and I. A. Aksay, *Appl. Opt.* **49**, 6689 (2010).
- ⁹R. Huang and Z. G. Suo, *Proc. R. Soc. London, Ser. A* **468**, 1014 (2012).
- ¹⁰R. E. Pelrine, R. D. Kornbluh, and J. P. Joseph, *Sens. Actuators, A* **64**, 77 (1998).
- ¹¹F. Carpi, P. Chiarelli, A. Mazzoldi, and D. De Rossi, *Sens. Actuators, A* **107**, 85 (2003).
- ¹²S. Yun, X. F. Niu, Z. B. Yu, W. L. Hu, P. Brochu, and Q. B. Pei, *Adv. Mater.* **24**, 1321 (2012).
- ¹³S. M. Ha, W. Yuan, Q. B. Pei, R. Pelrine, and S. Stanford, *Adv. Mater.* **18**, 887 (2006).
- ¹⁴G. Kofod, P. Sommer-Larsen, R. Kronbluh, and R. Pelrine, *J. Intell. Mater. Syst. Struct.* **14**, 787 (2003).
- ¹⁵A. N. Gent, *Rubber Chem. Technol.* **69**, 59 (1996).
- ¹⁶Z. G. Suo, *Acta Mech. Solida Sinica* **23**, 549 (2010).
- ¹⁷J. Zhu, H. Stoyanov, G. Kofod, and Z. G. Suo, *J. Appl. Phys.* **108**, 074113 (2010).
- ¹⁸M. Kollasche, J. Zhu, Z. G. Suo, and G. Kofod, *Phys. Rev. E* **85**, 051801 (2012).
- ¹⁹S. J. A. Koh, T. F. Li, J. X. Zhou, X. H. Zhao, W. Hong, J. Zhu, and Z. G. Suo, *J. Polym. Sci. Pol. Phys.* **49**, 504 (2011).
- ²⁰X. H. Zhao, W. Hong, and Z. G. Suo, *Phys. Rev. B* **76**, 134113 (2007).
- ²¹C. Keplinger, M. Kaltenbrunner, N. Arnold, and S. Bauer, *Appl. Phys. Lett.* **92**, 192903 (2008).
- ²²J. S. Plante and S. Dubowsky, *Sens. Actuators, A* **137**, 96 (2007).
- ²³J. S. Huang, T. F. Li, C. C. Foo, J. Zhu, D. R. Clarke, and Z. G. Suo, *Appl. Phys. Lett.* **100**, 041911 (2012).
- ²⁴J. S. Plante and S. Dubowsky, *Int. J. Solids Struct.* **43**, 7727 (2006).
- ²⁵C. C. Foo, S. Cai, S. J. A. Koh, S. Bauer, and Z. G. Suo, *J. Appl. Phys.* **111**, 034102 (2012).
- ²⁶See supplementary material at <http://dx.doi.org/10.1063/1.4748114> for experimental details.